Steerable filtering using novel circular harmonic functions with application to edge detection

Papari, Giuseppe; Campisi, Patrizio; Petkov, Nicolai

Link to publication in University of Groningen/UMCG research database

Steerable filtering using novel circular harmonic functions with application to edge detection

Giuseppe Papari*, Patrizio Campisi**, Nicolai Petkov*

* Institute of Mathematics and Computing Science, University of Groningen
** Dipartimento di Elettronica Applicata, Universita' degli Studi Roma Tre, Roma, Italy

Abstract—In this paper, we perform approximate steering of the elongated 2D Hermite-Gauss functions with respect to rotations and provide a compact analytical expressions for the related basis functions. A special notation introduced here considerably simplifies the derivation and unifies the cases of even and odd indices. The proposed filters are applied to edge detection. Quantitative analysis shows a performance increase of about 12.5% in terms of the Pratt's figure of merit with respect to the well-established Gaussian gradient proposed by Canny.

Keywords-Edge detection; Hermite-Gauss wavelets; Steerable filters

I. Introduction

The concept of *steerability* has been introduced in [1]. Specifically, a set of filters depending on a continuous parameter is steerable if it can be expressed as a linear combination of fixed basis functions. The convolution of an image with a steerable filter can be evaluated exactly for any value the concerned parameter, by means of convolutions with each basis function [1]. Moreover, integrals and derivatives with respect to the parameters can be evaluated efficiently by acting directly on the coefficients. Steerable filtering has been successfully applied in several areas of image processing, such as feature detection [2]–[6], texture modeling [7], denoising [8], [9], or invariants theory [10], [11].

When a filter is not steerable, approximate steering is performed by looking for an exactly steerable template which approximates the original family of filters. This is usually done by deploying orthogonal bases, thus providing the most compact approximation [3], [6], [12]. However, as pointed out in [3] closed forms of the resulting basis functions are hardly found and numerical solutions are often deployed.

In this paper, we provide a closed form of the basis functions which steer 2D Hermite-Gauss functions with respect to rotations, which are circular harmonic functions (CHF). We also apply the proposed filters to the problem of edge detection and validate the method with a broad range of experimental results.

II. Background

In this section, we briefly recall the definition of steerable filters and of the 2D Hermite-Gauss functions.
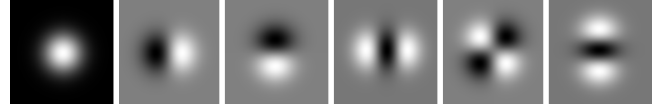

Figure 1. From left to right: 2D Hermite-Gauss filters of orders, respectively, (0,0), (1,0), (0,1), (2,0), (1,1), and (0,2).

A. Steerable filters

A family of filters $F(\mathbf{r}, \mathbf{\Lambda})$ which continuously depends on the parameter $\mathbf{\Lambda}$ is *steerable* if it can be expressed as linear combination of basis $V_s(\mathbf{r})$ with coefficients $a_s(\mathbf{\Lambda})$:

$$F(\mathbf{r}, \mathbf{\Lambda}) = \sum_{s=1}^{N} a_s(\mathbf{\Lambda}) V_s(\mathbf{r}) \qquad (1)$$

The convolution of an image $I(\mathbf{r})$ with a steerable filter is given by:

$$Y(\mathbf{r}, \mathbf{\Lambda}) \triangleq I(\mathbf{r}) \star F(\mathbf{r}, \mathbf{\Lambda}) = \sum_{s=1}^{N} a_s(\mathbf{\Lambda})[I(\mathbf{r}) \star V_s(\mathbf{r})]$$

Thus, once the convolutions $I(\mathbf{r}) \star V_s(\mathbf{r})$ are computed, $Y(\mathbf{r}, \mathbf{\Lambda})$ can be evaluated exactly for any $\mathbf{\Lambda}$.

Let us consider the case in which the concerned filters are rotated version of a fixed template $T(\mathbf{r})$, i.e., $\mathbf{\Lambda} = \theta$ and $F(\mathbf{r}, \theta) = T(R_\theta \mathbf{r})$, where R_θ is a rotation matrix of angle θ. We will express $\mathbf{r}$ in polar coordinates (ρ, ϕ). It can be shown that $F(\mathbf{r}, \theta)$ is steerable with respect to rotations iff the template $T(\mathbf{r})$ can be expressed as a linear combination of exponentials $e^{is\phi}$ with coefficients depending on ρ. Moreover, the coefficients $a_s(\theta)$ are simply $e^{is\theta}$ [1]. When $T(\rho, \phi)$ is not steerable, a steerable template which best approximates $T(\rho, \phi)$, is obtained by considering the first terms of the Fourier expansion of $T(\rho, \phi)$ with respect to the angular coordinate ϕ (singular value decomposition) [3].

B. Elongated 2D Hermite-Gauss filters

The 2D Hermite-Gauss (HG) filters are defined as

$$H^{m,n}(x,y) \triangleq \frac{1}{C^{(m,n)}} H_m(x) H_n(y) e^{-\frac{x^2+y^2}{2}}, \qquad (2)$$

where $C^{(m,n)} = \sqrt{2^{m+n}\pi m! n!}$ and $H_n(x) \triangleq e^{x^2}(-1)^n \frac{\mathrm{d}^n}{\mathrm{d}x^n}\left(e^{-x^2}\right)$ is the n-th order Hermite polynomial.

These filters are used to detect local features, such as edges and ridges and, more recently, for image compression [13], [14]. Examples of these filters for the orders 0, 1, and 2 are given in Fig. 1. Moreover, these filters are exactly steerable with respect to rotations and the basis functions are the well known Laguerre-Gauss harmonics [15].

In this paper, we are interested in the following template, where $\lambda > 0$ is a parameter:

$$T^{m,n}(x, y, \lambda) \triangleq H^{m,n}(\lambda x, \lambda^{-1}y) \qquad (3)$$

which is an elongated version of the HG defined above. One advantage of elongated filter is the possibility to go beyond Canny's limit in the tradeoff between good detection and good localization of a given feature [16]. Another advantage, illustrated in Fig. 2 concerns the possibility to discriminate between interesting features and noise by analyzing the response of the filter for different orientation. Specifically, let

$$Y^{m,n}(\mathbf{r}, \theta, \lambda) \triangleq I(\mathbf{r}) \star T^{m,n}(R_\theta \mathbf{r}, \lambda) \qquad (4)$$

be the result of the convolution of an image $I(\mathbf{r})$ with a rotated elongated HG filter. For a fixed point $\mathbf{r}$, this becomes a function of the sole θ, which is plotted in Fig. 2 for the case $(m, n) = (0, 1)$ and for $\lambda = 1$ and $\lambda = 2$. As we see, in the elongated case, the shape of the polar diagram changes considerably between an edge and a noisy input, thus discriminating between the two cases. In contrast, for the non-elongated case, such a discrimination is not possible.

Unfortunately, elongated HG filters are not exactly steerable with respect to rotations. Approximate steering has been performed in [3] for the orders $(0, 1)$ and $(0, 2)$ only, but only numerical solution have been provided. In the next section, we will extend the results given in [3] to provide a closed form of for the generic order (m, n).

III. STEERING THE 2D HG FILTERS

In this Section, we steer the template $T^{m,n}(x, y, \lambda)$ in the framework of singular value decomposition [3] by considering the following Fourier expansion:

$$T^{m,n}(\rho \cos \phi, \rho \sin \phi, \lambda) = \sum_{s=-\infty}^{\infty} V_s^{m,n}(\rho; \lambda)e^{is\phi}.$$

Let $\mathbf{U}^{m,n}(\rho; \lambda) \triangleq \{U_s^{m,n}(\rho; \lambda)\}_{s=-\infty}^{\infty}$ be a vector whose components are the required bases $U_s^{m,n}(\rho; \lambda)$. We need to evaluate the following integral:

$$\mathbf{U}^{m,n}(\rho; \lambda) = \\ = \frac{1}{2\pi} \int_0^{2\pi} H_{m,n}(\lambda \rho \cos \phi, \lambda^{-1} \rho \sin \phi)e^{-i\mathbf{k}\phi}\mathrm{d}\phi \qquad (5)$$

with $\mathbf{k} \triangleq [..., -2, -1, 0, 1, 2, ...]^T$

Let $x(\phi)$ be a periodic function with period 2π and let x_s its Fourier coefficients. As well known, the Fourier coefficients of the functions $u(\phi) \triangleq x(\phi)\cos\phi$ and $v(\phi) \triangleq$
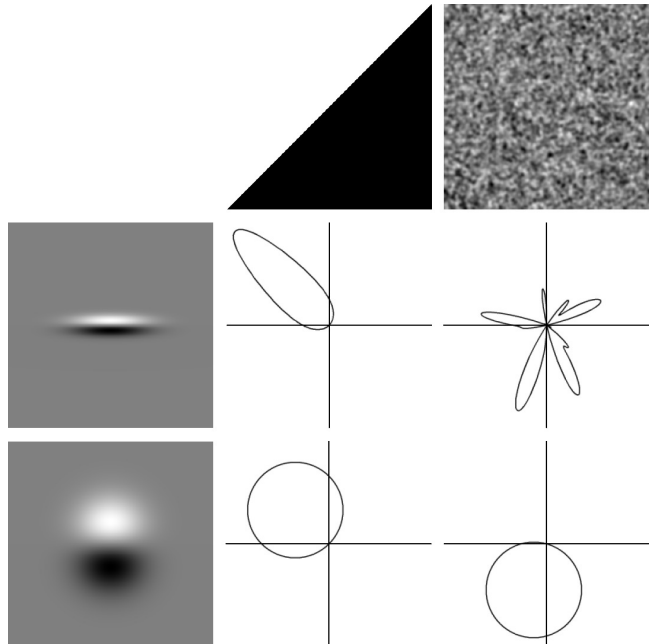

Figure 2. Top: an edge and a noisy input. Middle: the elongated filter $T^{0,1}(\mathbf{r}, \lambda)$, $\lambda = 2$ and the polar plot of the function $V^{0,1}(\mathbf{r}, \theta, \lambda)$ defined in (4), with $\mathbf{r}$ fixed at the center of the image. Bottom: the same for $\lambda = 1$.

$x(\phi)\sin\phi$ are, respectively, $u_s = (x_{s-1}+x_{s+1})/2$ and $v_s = (x_{s-1}-x_{s+1})/2i$. We introduce the vectors $\mathbf{x} \triangleq \{x_s\}_{s=-\infty}^{\infty}$, $\mathbf{u} \triangleq \{u_s\}_{s=-\infty}^{\infty}$, and $\mathbf{v} \triangleq \{v_s\}_{s=-\infty}^{\infty}$, and the *shifting matrix* $\mathcal{S}$ [1] , which is defined such that $\{\mathcal{S}\mathbf{a}\}_n = \{\mathbf{a}\}_{n+1}$ for every vector $\mathbf{a}$, where $\{\mathbf{a}\}_n$ denotes the n-th component of $\mathbf{a}$. Then, the above results can be rewritten as $\mathbf{u} = \mathcal{R}\mathbf{x}$ and $\mathbf{v} = \mathcal{I}\mathbf{x}$, with $\mathcal{R} \triangleq (\mathcal{S}^{-1} + \mathcal{S})/2$ and $\mathcal{I} \triangleq (\mathcal{S}^{-1} - \mathcal{S})/2i$. More in general, due to the linearity of the Fourier operator, the coefficients of the functions $x(\phi)P(\cos\phi)$ and $x(\phi)Q(\sin\phi)$ with P and Q polynomials, are equal to $P(\mathcal{R})\mathbf{x}$ and $Q(\mathcal{I})\mathbf{x}$. Therefore the evaluation of (5) reduces to the evaluation of $\mathbf{U}^{0,0}(\rho; \lambda)$ since we obtain:

$$\mathbf{U}^{m,n}(\rho; \lambda) = \\ = \frac{1}{C^{(m,n)}} H_m\left(\rho\lambda\mathcal{R}\right) H_n\left(\rho\lambda^{-1}\mathcal{I}\right)\mathbf{U}^{0,0}(\rho; \lambda) \qquad (6)$$

The integral (5) for $(m, n) = (0, 0)$ can be easily evaluated with basic calculus, by taking into account the well known result $\int_0^{2\pi} e^{x\cos u + iku}\mathrm{d}u = 2\pi I_n(x)$, where $I_n(x)$ is the n-th order modified Bessel function of the first type. Specifically, we have:

$$\mathbf{U}^{0,0}(\rho; \lambda) = e^{-\alpha\rho^2}\mathbf{I}\left(\beta\rho^2\right) \qquad (7)$$

[1]The matrix $\mathcal{S}$ has an unlimited number of elements. In general, operations with infinite matrices are expressed in terms of infinite series, therefore convergence problems may occur. However, since the matrix $\mathcal{S}$ has only one nonzero element per row, convergence is trivially guaranteed. Convergence allows to manipulate unlimited matrices with the ordinary algebraic rules.
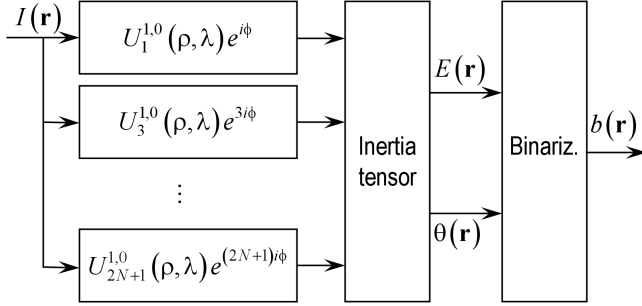
Figure 3. Proposed approach for edge detection.

with:

$$\mathbf{I}(z) \triangleq [..., 0, I_{-1}(z), 0, I_0(z), 0, I_1(z), 0, ...]^T \quad (8)$$

and $\alpha \triangleq (\lambda^{-2} + \lambda^2)/4$, $\beta \triangleq (\lambda^{-2} - \lambda^2)/4$.

Therefore, combining (6) and (7), we obtain

$$\mathbf{U}^{m,n}(\rho; \lambda) = \frac{e^{-\alpha\rho^2}}{C^{(m,n)}} H_m\left(\rho\lambda\mathcal{R}\right) H_n\left(\rho\lambda^{-1}\mathcal{I}\right) \mathbf{I}\left(\beta\rho^2\right)$$

which is the required closed form. As we see, the functions $U_s^{m,n}(\rho, \lambda)$ are linear combinations of modified Bessel functions, whose coefficients are expressed in terms of Hermite polynomials of $\lambda\rho$ and $\lambda^{-1}\rho$.

IV. Experimental Results

We now show some experimental results related to the application of the proposed CHF to edge detection. We follow the approach depicted in Fig. 3. To discriminate between edges and noise, we compute the inertia tensor of the polar diagram of Fig. 2 for each point of the input image. Specifically, we compute (i) edge strength $E_\lambda(\mathbf{r})$ as the difference between the maximum and the minimum eigenvalue of such inertia tensor, and (ii) local edge direction $\theta_\lambda(\mathbf{r})$ as the direction of the eigenvector that corresponds to the minimum eigenvalue. With basic algebra, it can be proved that $E_\lambda(\mathbf{r})$ and $\theta_\lambda(\mathbf{r})$ are, respectively, amplitude and phase of the following complex number:

$$Z(\mathbf{r}) \triangleq \sqrt{\sum_{s=-\infty}^{\infty} c_s(\mathbf{r})\overline{c_{s-2}(\mathbf{r})}} \quad (9)$$

where $\overline{z}$ indicates the complex conjugate of z, and with:

$$c_s(\mathbf{r}) \triangleq I(\mathbf{r}) \star U_s^{1,0}(\rho, \lambda)e^{i(2s+1)\phi} \quad (10)$$

An example of the edge strength $E_\lambda(\mathbf{r})$ is shown in Fig. 4 for $\lambda = 1$ and $\lambda = 2$. As we see, higher values of λ result in better edge localization and less noisy contours, especially in presence of texture. Moreover, large values of λ better preserve object contours, such as in the tusks of the elephant (marked by an arrow), and texture edges form structured chains of collinear edges; in contrast, for $\lambda = 1$ they only form meaningless random patterns. A larger set of examples
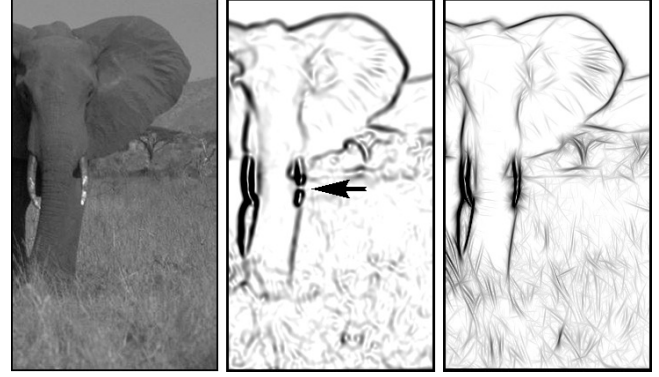

Figure 4. From left to right: Input image and edge strength $E_\lambda(\mathbf{r})$ for $\lambda = 1$ and $\lambda = 2$
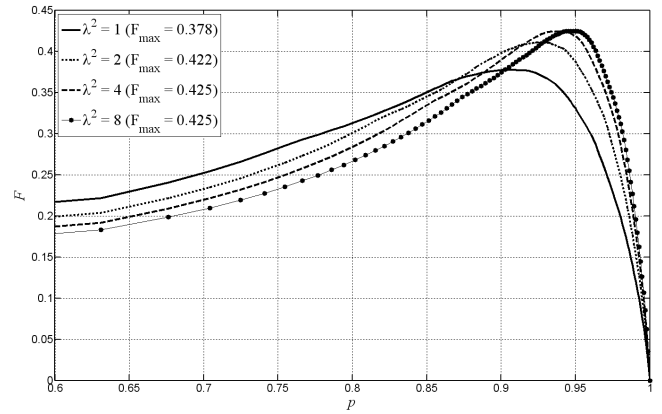

Figure 5. Performance of the proposed method, averaged on a set of 40 images, for different values of λ.

is available on line[2]. Finally, edges are detected as in [16] by applying non-maxima suppression and thresholding.

Finally, edges are detected as in [16] by applying non-maxima suppression and thresholding. To quantify the performance improvement that elongated filter offer over non-elongated ones, we have compared the detected contours with hand drawn ground truths. Similarity between our results and ground truths has been measured in terms of the well-established Pratt's figure of merit F [17]. The values of F, averaged over a set of 40 images, are plotted in Fig. 5 for different values of λ vs the fraction p of pixels that are rejected by thresholding. As we see, higher values of λ result in an improvement of about 12.5% in terms of F. We also observe a slow decay of the performance for $\lambda > 3$. This is due to numerical instability caused by the fact that for high values of λ the size of the filter orthogonally to the edge direction becomes less than half pixel

[2]http://www.cs.rug.nl/~imaging/ICPR2010

V. Summary and Conclusions

Elongated filters improve local detection of oriented features with respect to non-elongated ones in terms of a better compromise between noise rejection and localization accuracy. This makes the problem of steering such filters with respect to rotations particularly interesting in computer vision. However, finding the basis functions is a hard problem and only numerical solutions have been presented. In contrast, an analytic solution of the basis functions has been presented in this paper for steering with respect to rotation an important class of filters, namely the elongated 2D Hermite-Gauss functions. Moreover, the special notation introduced here, greatly simplifies the related maths and, in particular, unifies the cases of even and odd indices. The proposed filters are applied to the problem of edge detection. Quantitative analysis shows a performance increase of about 12.5% in terms of the Pratt's figure of merit with respect to the well-established non-elongated case.

References

[1] W. Freeman and E. Adelson, "The design and use of steerable filters," *IEEE Transactions on Pattern analysis and machine intelligence*, vol. 13, no. 9, pp. 891–906, 1991.

[2] P. Perona, "Steerable-scalable kernels for edge detection and junction analysis," *Image and Vision Computing*, vol. 10, no. 10, pp. 663–672, 1992.

[3] ——, "Deformable kernels for early vision," *IEEE Transactions on Pattern Analysis and Machine Intelligence*, vol. 17, no. 5, pp. 488–499, 1995.

[4] E. Simoncelli and H. Farid, "Steerable wedge filters for local orientation analysis," *IEEE transactions on Image Processing*, vol. 5, no. 9, pp. 1377–1382, 1996.

[5] R. Manduchi, P. Perona, and D. Shy, "Efficient deformable filter banks," *IEEE Transactions on Signal Processing*, vol. 46, no. 4, pp. 1168–1173, 1998.

[6] P. Teo and Y. Hel-Or, "Design of multiparameter steerable functions using cascade basis reduction," *IEEE Transactions on Pattern Analysis and Machine Intelligence*, vol. 21, no. 6, pp. 552–556, 1999.

[7] M. Do and M. Vetterli, "Rotation invariant texture characterization and retrieval using steerable wavelet-domain hidden markov models," *IEEE Transactions on Multimedia*, vol. 4, no. 4, pp. 517–527, 2002.

[8] J. Portilla, V. Strela, M. Wainwright, and E. Simoncelli, "Image denoising using scale mixtures of gaussians in the wavelet domain," *IEEE Transactions on Image processing*, vol. 12, no. 11, pp. 1338–1351, 2003.

[9] A. Bharath and J. Ng, "A steerable complex wavelet construction and its application to image denoising," *IEEE Transactions on Image Processing*, vol. 14, no. 7, pp. 948–959, 2005.

[10] L. Van Gool, T. Moons, E. Pauwels, and A. Oosterlinck, "Vision and lie's approach to invariance," *Image and vision computing*, vol. 13, no. 4, pp. 259–277, 1995.

[11] X. Shi, A. Castro, R. Manduchi, and R. Montgomery, "Rotational invariant operators based on steerable filter banks," *IEEE Signal Processing Letters*, vol. 13, no. 11, p. 684, 2006.

[12] G. Sommer, M. Michaelis, and R. Herpers, "The svd approach for steerable filter design," in *IEEE International Symposium on Circuits and Systems*, vol. 5, 1998, pp. 349–353.

[13] A. Refregier, "Shapelets - i. a method for image analysis," *Monthly notices of the Royal Astronomial society*, vol. 338, no. 1, pp. 35–47, 2003.

[14] R. Massey and A. Refregier, "Polar shapelets," *Monthly notices of the Royal Astronomial society*, vol. 363, no. 1, pp. 197–210, 2005.

[15] I. Kimel and L. Elias, "Relations between hermite and laguerre gaussian modes," *IEEE Journal of Quantum Electronics*, vol. 29, no. 9, pp. 2562–2567, 1993.

[16] J. Canny, "A computational approach to edge detection," *IEEE Transactions on Pattern Analysis and Machine Intelligence*, vol. 8, no. 6, pp. 679–698, 1986.

[17] I. Abdou and W. Pratt, "Quantitative design and evaluation of enhancement/thresholding edge detectors," *Proceedings of the IEEE*, vol. 67, no. 5, pp. 753–763, 1979.